# Lattice-Dictated Conformers in Bis(pyrazolyl)pyridine-Based Iron(II) Complexes: Mössbauer, NMR, and Magnetic Studies

**P. Manikandan,[†] K. Padmakumar,[†,‡] K. R. Justin Thomas,[†] B. Varghese,[†] H. Onodera,[§] and P. T. Manoharan*,[†,∥]**

Department of Chemistry and Regional Sophisticated Instrumentation Centre, Indian Institute of Technology/Madras, Chennai-600 036, India, and Institute for Materials Research, Tohoku University, Sendai 980-8577, Japan

*Received June 18, 2001*

Iron(II) complexes $[FeL_2](ClO_4)_2 \cdot CH_3CN$, $[FeL_2](BPh_4)_2 \cdot 2CH_3CN$, and $[FeL_2](PF_6)_2$ with an $FeN_6$ chromophore of the same ligand L (2,6-bis(3,5-dimethylpyrazol-1-ylmethyl)pyridine) and differing counterions have been made and their crystal and molecular structures determined. The first two crystallized in triclinic space group $P\bar{1}$, and the third, with $PF_6^-$ anion in *Ibca* space group. The $FeL_2$ complex ions in all lattices have similarly distorted octahedral geometry. Variable-temperature Mössbauer spectra of $[FeL_2](ClO_4)_2 \cdot CH_3CN$ and $[FeL_2](PF_6)_2$ measured in the temperature range 1.7−300 K reveal temperature-dependent populations of two different spin states with increased amount of low-spin form at high temperatures, a phenomenon unlike the normal spin crossover behavior; this abnormal behavior is interpreted here as due to the presence of two different conformations. It is very interesting to note that the two different compounds have similar spectra, Mössbauer parameters, and temperature dependence. But the variable-temperature Mössbauer spectra of $[FeL_2](BPh_4)_2 \cdot 2CH_3CN$ in the range 20−300 K do not show the presence of such different species but exhibit a clear phase transition at ∼200 K. This phase transition is further supported by SQUID measurements. The results of variable-temperature $^1H$ NMR in $CD_3CN$ and the solution susceptibility measurement of all complexes also support the presence of high-spin and low-spin forms in solution. Hence, the complex ion $[FeL_2]^{2+}$ exhibits a thermally driven interconversion between low-spin and a high-spin structural forms—a phenomenon observed in the solid and solution states due to ligand dynamics. This is not due to the well-known spin crossover phenomenon. These results are compared with the case of normal spin crossover seen in $[FeL'_2](ClO_4)_2$ (L' = 2,6-(bis(pyrazol-1-ylmethyl)pyridine)).

## Introduction

Studies on spin-crossover systems have been a very fascinating subject for the past three decades since many chemically and biologically significant transformations of Fe(II) complexes are accompanied by a change in the metal ion spin state. Extensive investigations on complexes which exhibit "spin equilibrium" behavior have been carried out, since such spin-state change drastically alters the strength of ligand−metal ion interactions and hence the chemical properties of the complex.[1−6] Spin crossover behavior in Fe(II) complexes, involving transition between high-spin ($^5T_2$, $S = 2$) and low-spin ($^1A_1$, $S = 0$) states, is an actively studied phenomenon. This spin crossover is mainly a cooperative phenomenon which passes the information from one molecule or one state of the molecule to the other.[7,8] The first ever developed Fe(II) spin crossover system dates back to the 1960s when $[Fe(phen)_2(NCS)_2]$ (phen = 1,10-phenanthroline) was synthesized.[9] Thereafter the research in this field was quite contagious.[10−23]

* To whom all correspondence should be addressed. E-mail: ptm@magnet.iitm.ernet.in. Fax: 91-044-2350509, 2352545.

† Indian Institute of Technology/Madras.

‡ Visiting Fellow JNCASR, Bangalore.

§ Tohoku University.

∥ Honorary Professor, Jawaharlal Nehru Centre for Advanced Scientific Research, Bangalore, India.

(1) Barefield, E. K.; Busch, D. H.; Nelson, S. M. *Q. Rev., Chem. Soc.* **1968,** *22,* 457.
(2) König, V. E. *Ber. Bunsen-Ges. Phys. Chem.* **1972,** *76,* 975.
(3) Hall, G. R.; Hendrickson, D. N. *Inorg. Chem.* **1976,** *15,* 607.
(4) Katz, B. A.; Strouse, C. E. *J. Am. Chem. Soc.* **1979,** *101,* 6214.
(5) Wilson, L. J.; Georges, D.; Hoselton, M. A. *Inorg. Chem.* **1975,** *14,* 2968.
(6) Sinn, E.; Sim, G.; Dose, E. V.; Tweedle, M. F.; Wilson, L. J. *J. Am. Chem. Soc.* **1978,** *100,* 3375.
(7) Addison, A. W.; Burman, S.; Wahlgren, C. G.; Rajan, O. A.; Rowe, T. M.; Sinn, E. *J. Chem. Soc., Dalton Trans.* **1987,** 2621.
(8) Wilson, L. J.; Tweedle, M. F. *J. Am. Chem. Soc.* **1976,** *98,* 4825.
(9) Baker, W. A.; Bobonich, H. M. *Inorg. Chem.* **1964,** *3,* 118.
(10) Christiansen, L.; Hendrickson, D. N.; Toftlund, H.; Wison, S. R.; Xie, C. L. *Inorg. Chem.* **1986,** *25,* 2813.
(11) Gütlich, P.; Hauser, A.; Spiering, H. *Angew. Chem., Int. Ed. Engl.* **1994,** *33,* 2024.
(12) Goodwin, H. A.; Kucharski, E. S.; Wales, A. H. *Aust. J. Chem.* **1983,** *36,* 1115.
(13) Eichhorn, D. M.; Armstrong, W. H. *Inorg. Chem.* **1990,** *29,* 3607.
(14) Figg, D. C.; Herber, R. H.; Potenza, J. A. *Inorg. Chem.* **1992,** *31,* 2111.
(15) Katz, B. A.; Strouse, C. E. *Inorg. Chem.* **1980,** *19,* 658.
(16) Greenaway, A. M.; Sinn, E. *J. Am. Chem. Soc.* **1978,** *100,* 8080.
(17) Wiehl, L.; Kiel, G.; Köhler, C. P.; Spiering, H.; Gütlich, P. *Inorg. Chem.* **1986,** *25,* 1565.
(18) Baker, A. T.; Goodwin, H. A.; Rae, A. D. *Inorg. Chem.* **1987,** *26,* 3513.
(19) Bousseksou, A.; Verelst, M.; Constant-Machado, H.; Lemercier, G.; Tuchagues, J. P.; Varret, F. *Inorg. Chem.* **1996,** *35,* 110.
(20) Ozarowski, A.; McGarvey, B. R.; Sarkar, A. B.; Drake, J. E. *Inorg. Chem.* **1988,** *27,* 628.
(21) Oliver, J. D.; Mullica, D. F.; Hutchinson, B. B.; Milligan, W. O. *Inorg. Chem.* **1980,** *19,* 165.
(22) Gallois, B.; Real, J. A.; Hauw, C.; Zarembowitch, J. *Inorg. Chem.* **1990,** *29,* 1152.
(23) Baker, A. J.; Ferguson, N. J.; Goodwin, H. A.; Rae, A. D. *Aust. J. Chem.* **1989,** *42,* 623.

We report here the crystal and molecular structure of three iron(II) complexes of a tridentate nitrogen donor ligand, 2,6-bis(3,5-dimethylpyrazol-1-ylmethyl)pyridine, and their detailed spectroscopic and magnetic investigations using variable-temperature Mössbauer spectroscopy in the solid state, magnetic measurements in the solid and solution states, and variable-temperature $^1$H NMR in solution. We have also carried out variable-temperature $^1$H NMR and magnetic susceptibility measurements in solution using the Evans method for [FeL′$_2$]-(ClO$_4$)$_2$ (L′ = 2,6-bis(pyrazol-1-ylmethyl)pyridine) which undergoes normal spin crossover, for a fruitful comparison. Although many Fe(II) compounds including the latter are known to exhibit the usual thermal spin crossover characteristics, two of the Fe(II) complexes reported here exhibit fully high spin characteristics at low temperatures, but on increasing the temperature, a new conformer probably with a low-spin form slowly develops its population to ~40% at ambient temperature. It must, however, be noted that Mahapatra and Mukherjee[24,25] have observed only a normal spin crossover in [FeL′$_2$](ClO$_4$)$_2$. The other Fe(II) complex of the same ligand L, with BPh$_4$ counterions, exhibits an interesting phase transition at ~200 K but exists as high-spin species throughout the temperature range.

## Experimental Section

$^1$H NMR spectra were recorded on a JEOL-GSX 400 spectrometer. Chemical shifts of the complex were referenced to tetramethylsilane (TMS). Variable-temperature NMR measurements were carried out in the temperature region 233−333 K using the JEOL variable-temperature controller. Magnetic measurements were carried out on a powder sample at a field of 0.1−1 T using a SQUID magnetometer operating in the temperature range 4.2−300 K. The error in the temperature was ±0.2 K, and that in the susceptibility was within 1%. The magnetic susceptibility was corrected for underlying diamagnetism using Pascal constants. Molar susceptibilities are given in m$^3$ mol$^{-1}$; magnetic moments were calculated according to the relation $\mu = 2.828\ (\chi_m T)^{1/2}$. Magnetic susceptibility measurements in solution were made using a modified Evans method.[26] The coaxial NMR tube contains pure acetonitrile solvent while the outer tube contains the iron complex dissolved in acetonitrile. The methyl protons of the acetonitrile in the inner and outer tubes show different chemical shifts. This separation in chemical shifts ($\Delta\nu$) was monitored with temperature, and it is considered as a paramagnetic shift. Initial Mössbauer measurements were made using the Canberra S-100 Mössbauer spectrometer fitted with a Wissel constant acceleration drive. The spectrum was recorded with a 512 multichannel analyzer. The source was $^{57}$Co/Pd (Amersham 50 mCi). The variable-temperature measurements were done in another instrument where a constant-acceleration (Wissel) type Mössbauer spectrometer together with a 1024-channel analyzer operating in the time scale mode was used. The standard γ-ray source $^{57}$Co/Rh (Amersham 25 mCi) was kept at room temperature for all measurements. The velocity corresponding to each channel was calibrated with the known spectrum of the metallic iron, and the isomer shifts reported here are with respect to α-Fe at room temperature. All low-temperature spectra were collected using a helium bath cryostat. The Mössbauer spectra were analyzed with computer programs using a Lorentzian line shape.

**Preparation.** All the solvents used were rigorously purified and dried prior to use. Other chemicals were purchased either from Aldrich Co. or locally and were pure enough for the synthesis. The Schlenk technique was used in the preparation of the Fe(II) complexes. 2,6-Bis(3,5-dimethylpyrazol-1-ylmethyl)pyridine (L) and 2,6-bis(pyrazol-1-ylmethyl)pyridine (L′) were prepared as reported in the literature.[24,27]

**[FeL$_2$](ClO$_4$)$_2$·CH$_3$CN (1).** The synthesis of the complex was accomplished following a previously published method.[25] To the deoxygenated methanolic solution containing 363 mg (1 mmol) of Fe-(ClO$_4$)$_2$·6H$_2$O was added 590 mg (2 mmol) of L with constant stirring; an immediate yellow precipitation resulted. The precipitate was filtered out and washed several times with 80% methanol to ensure the complete removal of any unreacted starting materials if present. The yield was 95%. The product was recrystallized from deoxygenated acetonitrile. Anal. Calcd: C, 48.77; H, 5.11; N, 17.38. Found: C, 48.52; H, 5.13; N, 17.52.

**[FeL$_2$](BPh$_4$)$_2$·2CH$_3$CN (2).** An acetonitrile solution of 88.66 mg (0.1 mmol) of the above complex [FeL$_2$](ClO$_4$)$_2$(CH$_3$CN) was added to 68.45 mg (0.2 mmol) of NaBPh$_4$ with constant stirring. The solution was allowed to stir for 0.5 h, and the solvent was evaporated. The crude product was washed many times with methanol−water (1:1), dried, and recrystallized from acetonitrile to give faint yellow prismatic crystals. The yield was 92%. Anal. Calcd: C, 76.07; H, 6.46; N, 11.62. Found: C, 76.12; H, 6.41; N, 11.70.

**[FeL$_2$](PF$_6$)$_2$ (3).** These crystals were made in a manner similar to that for **2** by using NaPF$_6$ in place of NaBPh$_4$. Anal. Calcd: C, 43.6; H, 4.52; N, 14.96. Found: C, 43.78; H, 4.65; N, 14.81.

**X-ray Data Collection and Structure Refinement.** Well-grown single crystals of appropriate size were selected for structure determination and sealed in a Lindemann tube, due to their propensity for solvent loss. The cell dimensions were obtained from the least-squares refinement of the 25 reflections. The complete data were collected at room temperature on an Enraf-Nonius CAD4 automatic four-circle diffractometer. The data were corrected for Lorentz and polarization effects, and an absorption correction was applied on the basis of ψ-scans.

The structures were solved by direct methods (SHELXS86),[28] and refinement was carried out by the full-matrix least-squares calculation.[29] Hydrogen atom positions were fixed on geometrically calculated positions and allowed to ride on their respective carrier atoms with isotropic thermal parameters of the parent atoms. The thermal parameters of the non-hydrogen atoms were anisotropically refined. The high residual density was located around perchlorate ions and the acetonitrile solvent molecules, which indicated slight disorder of the oxygen atoms of the perchlorate ions and diffused nature of the CH$_3$CN. However, the perchlorates were modeled satisfactorily without considering this slight disorder. The final convergence was achieved with $R$ = 0.0505, 0.0542, and 0.0563 respectively for **1**−**3**.

## Results and Discussion

The syntheses of the ligand and the complexes were accomplished in a straightforward manner by adopting routine procedures.[27] Elemental analyses confirm the formation of ML$_2$ complexes. There is no apparent sign of aerial oxidation in the solid state for an appreciable period of exposure to air except loss of crystallinity in the cases of **1** and **2**. However, the solution exposed to air for a long time gradually turns brown, presumably due to the formation of Fe(III). So when we deal with solutions, adequate care has to be taken to avoid any oxidation.

**Description of Structures.** Table 1 summarizes the experimental crystal data for **1**−**3,** and their selected bond lengths and bond angles are given in Table 2. The molecular structures of complexes **1**−**3** are displayed in Figures 1−3. The asymmetric units in **1** and **2** consist of the FeL$_2$ cation, two corresponding anions, and one/two CH$_3$CN molecules of crystallization. Compound **3** has similar asymmetric units but is free from solvent molecule. In all three compounds, (i) two molecules of the nitrogen donor tridentate ligand, L, are coordinated to Fe-(II) to form a distorted octahedral complex and (ii) a mean plane formed by three coordinated nitrogens of one ligand with Fe is

(24) Mahapatra, S.; Mukherjee, R. *J. Chem. Soc., Dalton Trans.* **1993**, 3723.
(25) Mahapatra, S.; Mukherjee, R. *Polyhedron* **1993**, *12*, 1603.
(26) Sandip, K. S. *J. Magn. Reson.* **1989**, *82*, 169.
(27) Manikandan, P.; Varghese, B.; Manoharan, P. T. *J. Chem. Soc., Dalton Trans.* **1996**, 371.

(28) Sheldrick, G. M. *Acta Crystallogr.* **1990**, *A46*, 467.
(29) Sheldrick, G. M. SHELXL-92, A Program for the Crystal Structure Refinement, University of Göttingen, Göttingen, Germany.

**Table 1.** Summary of Crystal Data and Data Collection Parameters for [FeL$_2$](ClO$_4$)$_2$·CH$_3$CN, [FeL$_2$](BPh$_4$)$_2$·2CH$_3$CN, and [FeL$_2$](PF$_6$)$_2$

| chem formula | C$_{36}$H$_{45}$Cl$_2$FeN$_{11}$O$_8$ (**1**) | C$_{86}$H$_{88}$B$_2$FeN$_{12}$ (**2**) | C$_{34}$H$_{42}$F$_{12}$FeN$_{10}$P$_2$ (**3**) |
|---|---|---|---|
| fw | 886.58 | 1367.15 | 936.57 |
| temp, K | 293(2) | 293(2) | 293(2) |
| $\lambda$, Å | 0.710 73 | 0.710 73 | 0.710 73 |
| space group | $P\bar{1}$ | $P\bar{1}$ | Ibca |
| $a$, Å | 11.125(9) | 11.444(3) | 12.6452(10) |
| $b$, Å | 11.144(9) | 16.799(8) | 15.361(3) |
| $c$, Å | 18.698(6) | 19.801(6) | 42.412(5) |
| $\alpha$, deg | 90.93(4) | 90.45(3) | 90.0 |
| $\beta$, deg | 92.62(6) | 91.59(2) | 90.0 |
| $\gamma$, deg | 114.6(4) | 94.28(3) | 90.0 |
| $V$, Å$^3$ | 2104(27) | 3795(2) | 8239(2) |
| $Z$ | 2 | 2 | 8 |
| $\rho_{calc}$ (g/cm$^3$) | 1.400 | 1.197 | 1.510 |
| $\mu_{Mo}$ (mm$^{-1}$) | 0.548 | 0.252 | 0.538 |
| $R(F_o)^a$ | 0.0732 | 0.1078 | 0.0950 |
| $R_w(F_o^2)^b$ | 0.1472 | 0.1696 | 0.2033 |

$^a$ $R(F) = \sum||F_o| - |F_c||/\sum F_o$. $^b$ $R_w(F_o^2) = [\sum[w(|F_o|^2 - |F_c|^2)]^2/\sum(w|F_o|^2)^2]^{1/2}$, where $w = 1/[\sigma^2(F_o^2) + (0.066P)^2 + 2.6P]$ and $P = (\max(F_o^2, 0) + 2F_c^2)/3$.

**Table 2.** Selected Bond Lengths (Å) and Angles (deg.) for [FeL$_2$](ClO$_4$)$_2$·CH$_3$CN, [FeL$_2$](BPh$_4$)$_2$·2CH$_3$CN, and [FeL$_2$](PF$_6$)$_2$

| [FeL$_2$](ClO$_4$)$_2$·CH$_3$CN (**1**) | | [FeL$_2$](BPh$_4$)$_2$·2CH$_3$CN (**2**) | | [FeL$_2$](PF$_6$)$_2$ (**3**) | |
|---|---|---|---|---|---|
| | | Bond Distances (Å) | | | |
| Fe−N(1) | 2.250(5) | Fe−N(1) | 2.251(3) | Fe−N(3)′ | 2.208(4) |
| Fe−N(3) | 2.218(5) | Fe−N(3) | 2.245(3) | Fe−N(3) | 2.208(4) |
| Fe−N(5) | 2.215(5) | Fe−N(5) | 2.235(3) | Fe−N(1)′ | 2.209(3) |
| Fe−N(6) | 2.241(5) | Fe−N(6) | 2.241(3) | Fe−N(1) | 2.209(3) |
| Fe−N(8) | 2.186(8) | Fe−N(8) | 2.199(3) | Fe−N(2)′ | 2.229(4) |
| Fe−N(10) | 2.203(10) | Fe−N(10) | 2.208(3) | Fe−N(2) | 2.229(4) |
| | | Bond Angles (deg) | | | |
| N(3)−Fe−N(1) | 85.0(2) | N(3)−Fe−N(1) | 85.79(10) | N(3)′−Fe−N(3) | 95.1(2) |
| N(5)−Fe−N(1) | 85.5(2) | N(5)−Fe−N(1) | 86.15(10) | N(3)′−Fe−N(1)′ | 171.47(14) |
| N(5)−Fe−N(3) | 169.98(12) | N(5)−Fe−N(3) | 171.91(10) | N(3)−Fe−N(1)′ | 86.34(14) |
| N(6)−Fe−N(1) | 177.13(12) | N(6)−Fe−N(1) | 177.50(10) | N(3)′−Fe−N(1) | 86.34(14) |
| N(6)−Fe−N(3) | 93.3(2) | N(6)−Fe−N(3) | 96.43(10) | N(3)−Fe−N(1) | 171.47(14) |
| N(5)−Fe−N(6) | 96.4(2) | N(5)−Fe−N(6) | 91.63(10) | N(1)′−Fe−N(1) | 93.47(18) |
| N(8)−Fe−N(1) | 93.7(4) | N(8)−Fe−N(1) | 95.72(10) | N(3)′−Fe−N(2) | 93.65(14) |
| N(8)−Fe−N(3) | 95.25(14) | N(8)−Fe−N(3) | 92.21(11) | N(3)−Fe−N(2) | 85.53(14) |
| N(8)−Fe−N(5) | 88.43(14) | N(8)−Fe−N(5) | 87.85(11) | N(1)′−Fe−N(2) | 94.84(13) |
| N(8)−Fe−N(6) | 84.2(4) | N(8)−Fe−N(6) | 85.34(10) | N(1)−Fe−N(2) | 85.99(13) |
| N(8)−Fe−N(10) | 169.85(14) | N(8)−Fe−N(10) | 171.12(10) | N(3)−Fe−N(2) | 85.53(14) |
| N(10)−Fe−N(1) | 96.5(3) | N(10)−Fe−N(1) | 93.15(10) | N(3)′−Fe−N(2)′ | 93.65(14) |
| N(10)−Fe−N(3) | 85.6(2) | N(10)−Fe−N(3) | 88.03(11) | N(1)′−Fe−N(2)′ | 85.99(13) |
| N(10)−Fe−N(5) | 92.44(14) | N(10)−Fe−N(5) | 93.16(10) | N(1)−Fe−N(2)′ | 94.84(13) |
| N(10)−Fe−N(6) | 85.7(3) | N(10)−Fe−N(6) | 85.81(10) | N(2)−Fe−N(2)′ | 178.79(18) |
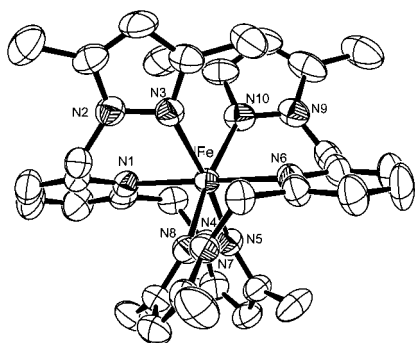


**Figure 1.** ZORTEP plot of the FeL$_2^{2+}$ cation of [FeL$_2$](ClO$_4$)$_2$·CH$_3$-CN. (Perchlorate ions, the acetonitrile molecule, and hydrogen atoms are omitted for clarity.)

approximately perpendicular to that of the other ligand. Of particular interest is a comparison of the geometry of the FeL$_2$ cation in the three unit cells. The ligand adopts a *mer* conformation about the central metal ion. The Fe−N bond lengths range from 2.186(8) to 2.250(5) Å in **1**, 2.199(3) to 2.251(3) Å in **2**, and 2.208(4) to 2.229(4) Å in **3** all of which are typically $r_{HS}$ at RT (room temperature).[17,30−32] The distortion
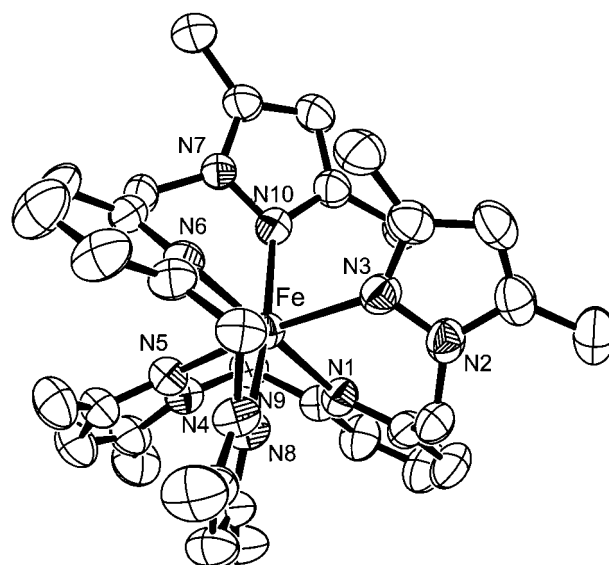


**Figure 2.** ZORTEP plot of the FeL$_2^{2+}$ cation of [FeL$_2$](BPh$_4$)$_2$·2CH$_3$-CN. (Tetraphenyborate ions, the acetonitrile molecule, and hydrogen atoms are omitted for clarity.)
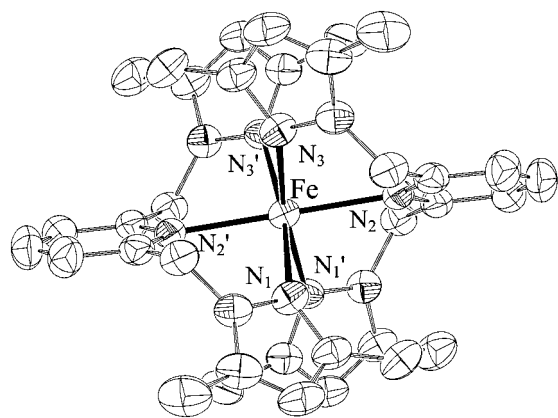
**Figure 3.** ZORTEP plot of the $FeL_2^{2+}$ cation of $[FeL_2](PF_6)$. (Hexafluorophoshate ions and hydrogen atoms are omitted for clarity.)

from octahedral geometry is maximum in **1** and minimum in **3**. The average differences between Fe−N(py) and Fe−N(pz) bond lengths in $FeL_2$ of **1**−**3** are 0.04, 0.02, and 0.02 Å, respectively. Also, the average of bond distances is the maximum for **2** and minimum for **3**. Both **1** and **3** are tetragonally elongated along Fe−N(Py) bonds while the geometry around the metal in **2** is tetragonally compressed, the equatorial plane being N(1)N(3)N-(5)N(6). In complex $[FeL_2](BPh_4)_2 \cdot 2CH_3CN$ the $BPh_4$ anions are isolating the iron center. All distances and angles in the tetraphenylborate anion appear normal. All the phenyl rings are essentially planar; the average C−C distance is 1.384 Å, and the average B−C distance is 1.650 Å. Such an isolation of $FeL_2$ present in **2** is rather restricted in **1** and **3**. The N−Fe−N bond angles vary from 84.2(4) to 177.13(12), 85.0(2) to 177.13(12), and 85.53(14) to 178.79(10)° respectively in crystals **1**−**3** indicating that there is not much of a difference between them. The mean planes of the pyridine rings of the two ligands in the $ClO_4^-$ lattice are tilted at an angle of 26.04°. The dihedral angles between the planes formed by the pyrazolyl groups within the two ligand molecules in the same complex **1** are 118.3 and 111.58°. The pyridine mean plane is tilted to adjacent pyrazolyl rings within a ligand at angles of 56.69 and 118.93° and 124.12 and 55.59°. Almost similar situations exist in **2** and **3**. Thus, the chelate rings in all complexes assume boat conformation.

No evidence exists for any alteration in the planarity of the pyridine and pyrazolyl rings of all complexes. In all complexes, there is no significant hydrogen-bonding network in the lattice. In addition, the solvent of crystallization, $CH_3CN$, in **1** and **2** plays no significant role other than acting as a space filler in these complexes.

**Mössbauer Spectroscopy.** The room-temperature Mössbauer spectrum of $[FeL_2](ClO_4)_2 \cdot CH_3CN$ had been reported earlier without much detail.[25] A similar complex, $[FeL(_2)(ClO_4)_2$, without the methyl substituents at the pyrazole ring of ligand was found to undergo normal spin crossover in the range from 300 to 77 K.[25] We report here the Mössbauer spectra of $[FeL_2]$-$(ClO_4)_2 \cdot CH_3CN$ recorded in the temperature range from 300 to 4.2 K (Figure 4). Throughout this temperature range there is a major quadrupole split component with an isomer shift of 1.16 mm/s and a quadrupole splitting of 3.1 mm/s at 4.2 K. The crowding of the ligand makes it a distorted octahedral molecule, which gives a large quadrupole coupling constant. The values are found to vary slightly with temperature as it is normally
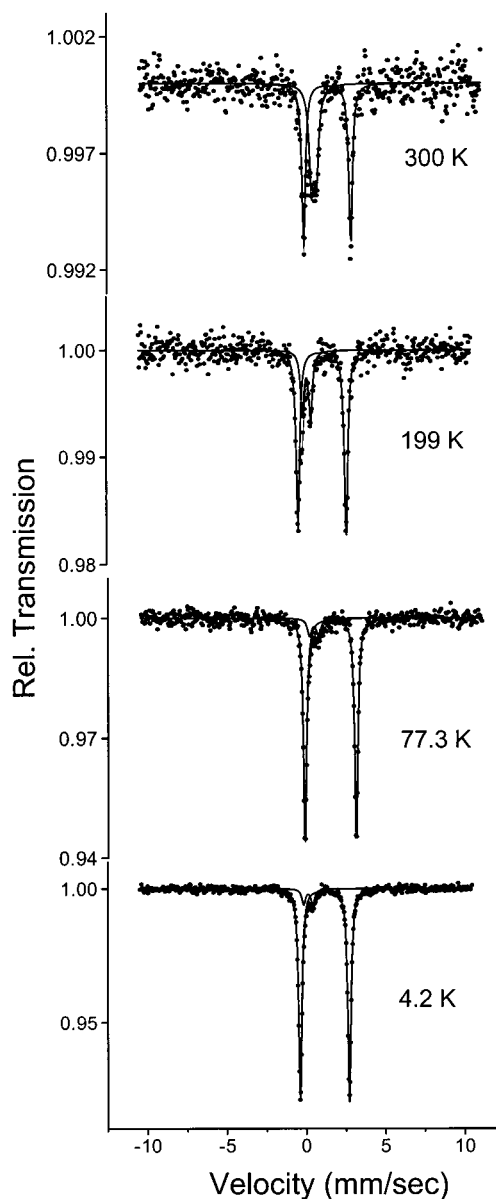


**Figure 4.** Mössbauer spectra of $[FeL_2](ClO_4)_2 \cdot CH_3CN$ in the temperature range 300−1.7 K.

expected for $Fe^{2+}$ high-spin complexes. All these indicate the presence of Fe(II) in the high-spin state. The values of the isomer shift and the quadrupole splitting are given in Table 3. At the lowest temperature, viz. 4.2 K, the spectrum is mainly due to this high-spin component with the presence of a small amount of a quadrupole doublet which has an isomer shift value of 0.116 mm/s (average) characteristic of low-spin Fe(II) with an intensity of 7.5% of the total. The intensity of this peak reaches a value of nearly 40.8% of the total integrated intensity at 300 K. This observation cannot be attributed to the presence of any low-spin impurity, since in such an eventuality the low-spin part of the spectrum should be present throughout the temperature region with approximately the same percentage of intensity.[33−35] In other words, the low spin to high spin ratios should remain constant at all temperatures although the relative areas may vary slightly due to the Debye−Waller factors of the two spin states.

(30) Hoselton, M. A.; Wilson, L. J.; Drago, R. S. *J. Am. Chem. Soc.* **1975**, *97*, 1722.
(31) Katz, B. A.; Strouse, C. E. *J. Am. Chem. Soc.* **1979**, *101*, 6214.
(32) Mikami-Kido, M.; Saito, Y. *Acta Crystallogr., Sect. B* **1982**, *38*, 452.

(33) Boukheddaden, K.; Varret, F. *Hyperfine Interact.* **1992**, *72*, 349.
(34) Claude, R.; Real, J. A.; Zarembowitch, J.; Kahn, O.; Ouahab, L.; Grandjean, D.; Boukheddaden, K.; Varret, F.; Dworkin, A. *Inorg. Chem.* **1990**, *29*, 4442.
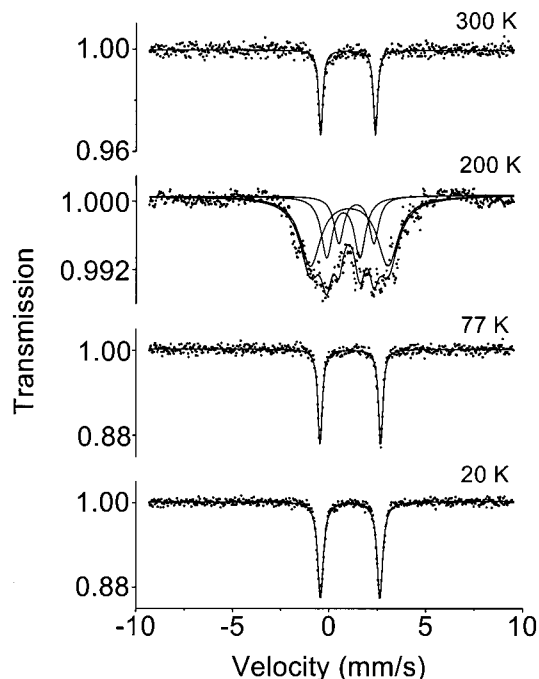(35) Konig, E.; Ritter, G.; Goodwin, H. A. *Chem. Phys.* **1973**, *1*, 17.

**Table 3.** Mössbauer Spectral Parameters of the Compound [FeL$_2$](ClO$_4$)$_2$·CH$_3$CN

| $T$, K | $\delta_1$,[a] mm/s | $\Delta E_Q$, mm/s | $\Gamma_1/2$, mm/s | $A_1$[a] | $\delta_2$, mm/s | $\Delta E_Q$, mm/s | $\Gamma_2/2$, mm/s | $A_2$[a] |
|---|---|---|---|---|---|---|---|---|
| 4.2 | 1.16(1) | 3.10(4) | 0.12(2) | 0.92(3) | 0.12(1) | 0.58(1) | 0.14(1) | 0.08(1) |
| 77.3 | 1.15(2) | 3.15(4) | 0.12(1) | 0.91(1) | 0.14(1) | 0.56(1) | 0.16(1) | 0.09(3) |
| 199 | 1.09(2) | 3.05(1) | 0.14(1) | 0.73(3) | 0.12(1) | 0.52(4) | 0.14(1) | 0.27(1) |
| 300 | 1.06(1) | 2.89(4) | 0.14(1) | 0.59(2) | 0.22(1) | 0.31(1) | 0.18(1) | 0.41(2) |

[a] With respect to Fe at room temperature. $A_1$ and $A_2$: relative transmissions.

If it is a problem due to differences in the recoil free fraction, then the intensity of the low-spin component should be more pronounced at lower temperatures. This is also opposite to the usual thermal spin crossover behavior. However, the existence of a "reverse" spin crossover is not possible due to entropy reasons and, hence, such a possibility is ruled out. A similar kind of observation has been earlier reported in a triaza complex with the percentage of the low-spin component increasing to 33% at ambient temperature.[10] The authors attributed this to the isomerization of the complex at high temperature. Again at high temperatures both isomers are present. They argue that at low temperatures there is a possibility for only one isomer being present due to restricted motion. A similar kind of explanation can be offered for the temperature-dependent behavior of the [FeL$_2$](ClO$_4$)$_2$·CH$_3$CN of this report. Here, one can also argue that the dynamics of the molecule or a dynamics attributed to the disposition of the ligand L alone can produce a small low-spin contribution at higher temperatures. The dynamics involving this ligand in Cu(I) complexes[27,36] have been already reported by us. The crystal structure of [FeL$_2$](ClO$_4$)$_2$·CH$_3$CN indicates that the ligands are arranged in *mer* conformation. A conversion of this *mer* conformation to *fac* conformation could alter the spin form. Furthermore, this interconversion with the preponderance of *mer* structure as shown in the crystal structure could occur at a frequency higher than that dictated by the diffraction of X-rays. It is very interesting to note from a very recent report[37] that two different Fe(II) sites in {Fe[HC(3,5-Me2pz)$_3$]$_2$}(BF$_4$)$_2$ detected clearly by Mössbauer at room temperature could not be revealed by the single-crystal X-ray diffraction studies. Similarly an earlier study of the Mössbauer spectra of Fe[B(3-isopropylpyrazol-1-yl)$_4$]$_2$ by Long and co-workers[38] reported the presence of Fe(II) in a pseudooctahedral environment where two doublets were observed even though the X-ray structural work[39] indicated the presence of only one crystallographically distinct iron(II) site. Hence, this lattice [FeL$_2$](ClO$_4$)$_2$·CH$_3$CN can be considered as an example of thermally driven interconversion of high-spin and low-spin forms promoted by the *mer* ↔ *fac* conformations. Another interpretation is that the chelation ring undergoes a change from boat at RT to chair at low temperature, creating two different structural forms.

When we replaced the ClO$_4^-$ counterion of [FeL$_2$](ClO$_4$)$_2$·CH$_3$-CN by BPh$_4^-$, we observe very interesting spectroscopic and magnetic results though we do not see any high-spin–low-spin isomers over a temperature region. The Mössbauer spectra of the [FeL$_2$](BPh$_4$)$_2$·2CH$_3$CN recorded at selective temperatures in range 300–20 K are given in Figure 5. Observation of a large quadrupole coupling constant throughout the temperature range (except at ∼200 K) indicates highly distorted octahedral

(36) Manikandan, P.; Moni, M. S.; Varghese, B.; Manoharan, P. T. *J. Chem. Soc., Dalton Trans.* **1998**, 3219.
(37) Reger, D. L.; Little, C. A.; Rheingold, A. L.; Lam, M.; Liable-Sands, L. M.; Rhagitan, B.; Concolino, T.; Mohan, A.; Long, G. J.; Briois, V.; Grandjean, F. *Inorg. Chem.* **2000**, *39*, 4674.
(38) Long, G. J.; Grandjean, F.; Trofimenko, S. *Inorg. Chem.* **1993**, *32*, 1055.
(39) Rheingold, A. Unpublished results.



**Figure 5.** Mössbauer spectra of [FeL$_2$](BPh$_4$)$_2$·2CH$_3$CN in the temperature range 300–20 K.

**Table 4.** Mössbauer Fitted Parameters for [FeL$_2$](BPh$_4$)$_2$·2CH$_3$CN

| $T$, K | $\delta$,[a] mm/s | $\Delta E_Q$, mm/s | $\Gamma/2$, mm/s | intensity (%) |
|---|---|---|---|---|
| 300 | 1.09 | 2.84 | 0.25 | 100 |
| | 1.14 | 4.03 | 1.30 | 56.1 |
| 200 | 0.85 | 1.72 | 0.70 | 26.3 |
| | 1.52 | 1.81 | 0.60 | 17.6 |
| 77 | 1.21 | 3.14 | 0.27 | 100 |
| 20 | 1.22 | 3.07 | 0.35 | 100 |

[a] With respect to natural Fe at room temperature.

geometry, which is indicative of the presence of Fe in the high-spin state with a +2 oxidation state. The values were found to vary slightly with temperature. The values of the chemical shift and the quadrupole splitting at different temperatures are given in Table 4.

The Mössbauer spectrum at 200 K, however, becomes very broad due to a first-order phase transition, and it could be easily fitted with three doublets with different chemical isomer shifts and quadrupole splittings (Table 4). Further support to this first-order phase transition comes from the solid-state magnetic moment measurements (vide infra) which show a cusp in the susceptibility at this same temperature. Though phase transition is confirmed both by Mössbauer results and magnetic measurements, the real evidence for the specifics of transformations comes from Mössbauer and to a lesser extent from the temperature-dependent FTIR spectrum. The phase transition may involve either a change in the chelating ring conformation from the boat form at room temperature (the crystal structure analysis of [FeL$_2$](BPh$_4$)$_2$·2CH$_3$CN proves the presence of a boat conformation for the chelation ring) to a chair form at low temperatures or *mer to fac* conformational change. At the

transition temperature of 200 K, three different structures are identifiable as a result of the process of conformational changes mentioned above. However, the structures present at this temperature appear to be some kind of metastable intermediates, totally different from those above and below 200 K. It may be pertinent to remind here of the dynamics involving this ligand in the case of Cu(I) complexes as investigated and reported earlier.[36] Similar behavior is noted in the case of bis(azido)-copper(II) complexes.[40] These three structures with differing isomer shifts and quadrupole coupling constants suggest possible routes or intermediates for a changeover from boat to chair conformation of chelating ring or from *mer-to-fac* in solid state on cooling as is evident from their differing $\delta$, $\Delta E_Q$, and $\Gamma/2$ values (Table 4). At this juncture, it is difficult to point which structure is formed first unless measurements are made at closer intervals of temperature, e.g. $\pm 1°$. A crystallographic measurement as a function of temperature around 200 K is in progress. One point, however, can be made that the species with large quadrupole splitting at 200 K is definitely a high-spin form, be it due to an extreme metastable form of boat or chair conformation. The other two lower quadrupole moment species reveal a tendency of $FeL_2$ to go toward a low-spin species, the structures of which are stabilized differently by different anions. The large line width $\Gamma/2$ for this fit of spectral data reveals considerable dynamics in progress as a result of phase transition, i.e. 0.60 to 1.30 mm/s compared to 0.25 to 0.35 mm/s for stable high- and low-temperature conformations. This large line width must have been caused by the dynamics of change from one to the other structures measured at 200 K in Table 4. The Mössbauer spectra at 210 and 190 K are slightly different from each other indicating that this phase transition is of first order from boat to chair or *mer-to-fac* conformation. The existence of such structures in other Cu(II) complexes with the same ligand or similar ligand like dipropylenetriamine (dpt) has been observed by us (Figure 6).[40] FTIR measurements of this complex ion in the solid state at 200 K show splitting of IR spectral lines revealing the presence of more than one structure at the temperature of phase transition. While the results on the lattices containing $ClO_4^-$ and $BPh_4^-$ anions are much different from each other, the Mössbauer spectra (Figure 7) of $[FeL_2](PF_6)_2$ revealed the same thermally driven interconversion of high-spin and low-spin forms in similarity to the perchlorate: (i) the percentage of low-spin form is nearly 39% at room temperature in comparison to 41% in the perchlorate lattice; (ii) the low-spin form has $\delta$ value and resolves into a doublet with a small $\Delta E_Q$ value in good similarity to the perchlorate lattice, characteristic of low-spin octahedral systems with trigonal or tetragonal distortion. Table 5 shows the Mössbauer parameters for compound **3**. A major point to note in all spectral data shown in Figures 4, 5, and 7 is that (i) there is a continuous increase in the Mössbauer absorption on decrease of the temperatures of solids **1**–**3** and (ii) there is a definite relative increase in the low-spin component with increase in temperature. These observations remove the possibility of $Fe^{3+}$ either in sample or on detector window. In a general sense, the spectral behavior appears to be also influenced by the size of the cation, i.e. $ClO_4^- < PF_6^- \ll BPh_4^-$, which in turn controls the volume space available for the $[FeL_2]^{2+}$ species to undergo restricted to unrestricted motional behavior (vide infra). Support for these observations also comes from susceptibility and NMR studies. That the "low-spin" form Mössbauer signals in **1** and **3** may be due to low-spin or high-
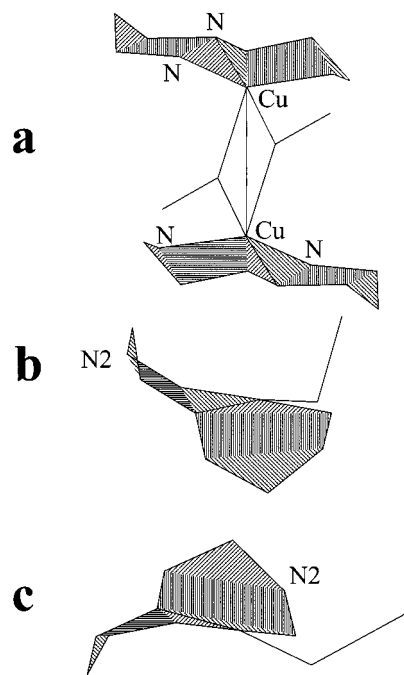


**Figure 6.** Presence of chair and boat conformations observed in two six-membered chelation rings: (top) chair forms in end-on $\mu$-1,1-diazido-bridged dipropylenetriamine (dpt) binuclear copper(II) complex; (middle and bottom) boat forms in the $CuLN_3$ moiety in a bis(azido) binuclear complex in two different but symmetry-related orientations.
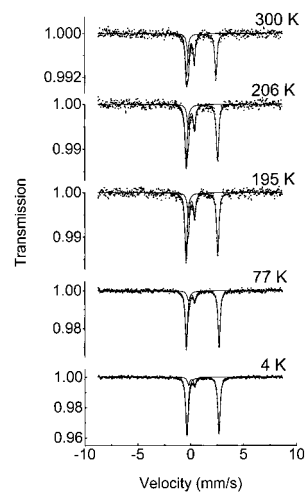


**Figure 7.** Mössbauer spectra of $[FeL_2](PF_6)$ in the temperature range 300–4.2 K.

spin Fe(III) species from possible oxidation of $FeL_2$ is ruled out by the total lack of EPR signals in the region of 77–300 K.
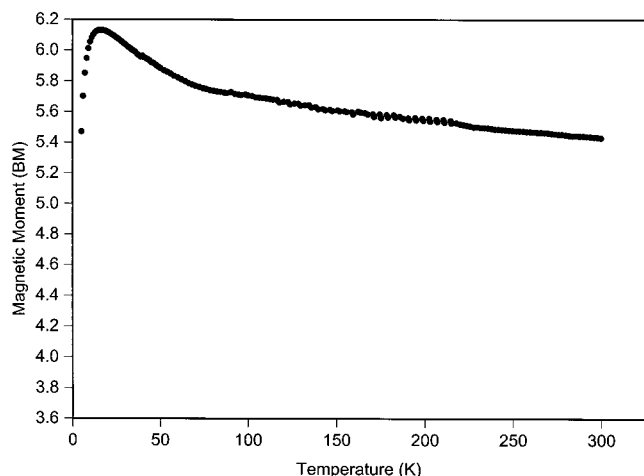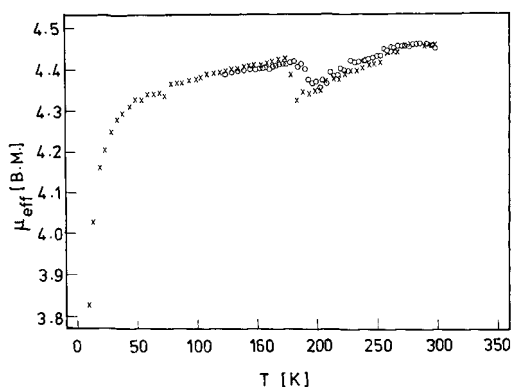
**Magnetic Properties.** The magnetic susceptibility measurements for $[FeL_2](ClO_4)_2 \cdot CH_3CN$ (Figure 8) were carried out using a SQUID magnetometer with an external magnetic field of the order of 1 T. First of all, a plot of $\chi^{-1}$ vs $T$ indicates zero value for the Weiss constant suggesting this compound to be a pure paramagnet, though the magnetic moment is of the order of 6.13 $\mu_B$ at 12 K which is larger than the normal spin-only value of 4.9 $\mu_B$ for high-spin iron(II) complexes with $S = 2$. The higher value must be due to the orbital and other contributions. However, the magnetic moment at higher temperatures clearly decreases in true correspondence with our Mössbauer results. Moreover the susceptibility data in the region of 120–200 K show scattering indicating the presence of motional behavior in the lattice. The stability of the susceptibility

(40) Manikandan, P.; Muthukumaran, R.; Justin Thomas, K. R.; Varghese B.; Chandramouli, G. V. R.; Manoharan, P. T. *Inorg. Chem.* **2001**, *40*, 2378.

**Table 5.** Mössbauer Spectral Parameters of the Compound $[FeL_2](PF_6)_2$

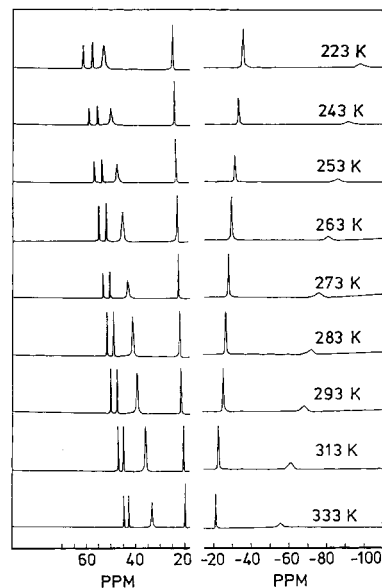| $T$, K | $\delta_1$,[a] mm/s | $\Delta E_Q^1$, mm/s | $\Gamma_1/2$, mm/s | $A_1$ | $\delta_2$, mm/s | $\Delta E_Q^2$, mm/s | $\Gamma_2/2$, mm/s | $A_2$ |
|---|---|---|---|---|---|---|---|---|
| 4.2 | 1.167 | 3.030 | 0.265 | 0.880 | 0.108 | 0.580 | 0.251 | 0.120 |
| 77.3 | 1.160 | 3.100 | 0.240 | 0.813 | 0.120 | 0.590 | 0.310 | 0.187 |
| 195 | 1.103 | 3.009 | 0.268 | 0.719 | 0.121 | 0.580 | 0.268 | 0.281 |
| 206 | 1.101 | 2.970 | 0.274 | 0.699 | 0.117 | 0.574 | 0.276 | 0.301 |
| RT | 1.050 | 2.790 | 0.258 | 0.610 | 0.110 | 0.550 | 0.258 | 0.390 |

[a] Wth respect to natural Fe at room temperature.



**Figure 8.** Variation of magnetic moment with temperature for $[FeL_2]$-$(ClO_4)_2 \cdot CH_3CN$ from SQUID susceptibility measurements.



**Figure 9.** Variation of magnetic moment with temperature for $[FeL_2]$-$(BPh_4)_2 \cdot 2CH_3CN$ from SQUID susceptibility measurements. ($\times$ and $\bigcirc$ refer to two different measurements.)



**Figure 10.** Variable-temperature $^1H$ NMR spectra of $[FeL_2](ClO_4)_2 \cdot CH_3-CN$ in the temperature range 233−333 K. Solvent: $CD_3CN$.

data below 100 K and above 200 K shows a smooth variation. This again can be attributed to the two-conformation model proposed above.

The magnetic susceptibility measurements for compound $[FeL_2](BPh_4)_2 \cdot 2CH_3CN$ have been carried out using a SQUID magnetometer with an external magnetic field of the order of 1000 G. The plot of the magnetic moment versus temperature is shown in Figure 9. It is very clear from this figure that the magnetic moment is of the order of 4.4 $\mu_B$ at 300 K which is slightly less than expected for a spin-only value, 4.9 $\mu_B$, for high-spin iron(II) complexes with $S = 2$. In addition, there is a "cusp" at about 200 K. This cusp confirmed by two different sets of measurements conforms to the findings by Mössbauer spectroscopy (vide infra) in the form of three Mössbauer doublets resolved out of a broadened spectral feature and substantiates our earlier interpretation of a phase transition from chair to boat conformation of chelation rings or a *mer-to-fac* transformation. Though this phase transition observed both by Mössbauer spectroscopy and magnetic susceptibility is essentially a solid-state phenomenon, the basic fluxional character

of the ligand is the cause behind this transformation. The $^5T_2$ ground state of $O_h$ split further by tetragonal/trigonal distortions and spin−orbit coupling creating energy levels separated by energies of the order of $kT$ (thermally populated in the high temperature range) causes the temperature-dependent magnetic moment for both compounds. Similarly a very large temperature-dependent magnetic moment at low temperatures is attributed to zero-field splitting of the high-spin Fe(II) ground state. A similar low-temperature magnetic behavior was observed for solid **1**. No magnetic measurements were made on $[FeL_2](PF_6)_2$ in view of its Mössbauer data being very similar to the perchlorate lattice.

**Nuclear Magnetic Resonance Study.** Solution $^1H$ NMR as a function of temperature throws light on changes of structure influenced by ligand fluxionality on the $FeL_2^{2+}$ ion, independent of the anion behavior and hence lattice packing effects. In other words, we can study the manifestation of the electronic energy states (associated with the $[FeL_2]^{2+}$ complex ion), especially the ones accessible to thermal population in the high-temperature regime up to 333 K, whereas Mössbauer spectroscopy becomes difficult above 300 K due to reduced recoil free fraction in addition to possible structural degradation in compound **1** due to the fear of losing $CH_3CN$ molecules from the lattice.

Proton NMR spectra of the ligand part of all three iron(II) complexes in $CD_3CN$ are identical and show peaks ranging from +48 to −63 ppm at 313 K (a little above room temperature) with respect to TMS characteristic of a species with organic ligands bound to a paramagnetic center. At the lowest possible temperature (233 K) in our variable-temperature $^1H$ NMR study, the peaks are spread out from +63 to −97 ppm with respect to TMS (Figure 10). As we increase the temperature, the resonance region keeps decreasing. At the highest measured temperature
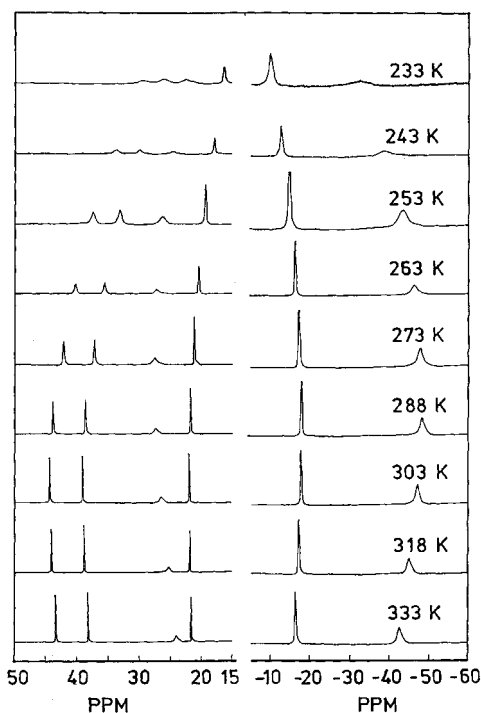
**Figure 11.** Variable-temperature $^1H$ NMR spectra of $[FeL'_2](ClO_4)_2$ in the temperature range 233−333 K. Solvent: $CD_3CN$.

of 333 K the resonance peaks are spread out from +45 to −54 ppm. These findings clearly not only support the thermally driven interconversion of low-spin and high-spin forms but also support increased population of low-spin conformer at higher temperatures. The room-temperature peaks at −63 and −23 ppm, respectively, have been assigned to the methylene protons which are found to be diastereotropic according to earlier work.[27,36]

The line width of the methylene protons was found to be inversely proportional to temperature. At high temperatures the sharpening of the NMR spectral lines arises from an increasing amount of low-spin isomer. As the temperature is lowered, the high-spin $^5T_2$ isomer gets increasingly populated producing more paramagnetic broadening. Sharpening of lines can also be attributed to faster interchange of the two conformers at high temperatures along with a higher population of the low-spin state while broadening at low temperature is due to slowing down of exchange of conformation along with increased population of high-spin-state species. It must, however, be mentioned that an increase in solvent viscosity on lowering the temperature also contributes to an increase in line width. In fact, the average moment responsible for the observed shifts should be due to the presence of these two possible isomers also in solution, since any conformational change (vide supra) should be easier in solution.

To lend credence to our conclusions of NMR results on $FeL_2^{2+}$, we also carried out variable-temperature $^1H$ NMR for another iron complex, $[FeL(_2(ClO_4)_2$, which undergoes normal spin cross over.[24,25] At the lowest possible temperature (233 K) the peaks are spread out from −30 to 32 ppm (Figure 11). As we increase the temperature, the spectral spread considerably increases and at 333 K the same peaks have a span of −43 to 43.5 ppm. There are two points worth noting: (i) The maximum spectral spreads occur at low temperatures for $[FeL_2]^{2+}$ but it is at high temperature for the $[FeL'_2]^{2+}$ ion. (ii) Such spectral spreads are larger for $[FeL_2]^{2+}$ than for $[FeL'_2]^{2+}$. In the case of $[FeL'_2]^{2+}$, on the basis of Mössbauer evidence, one can
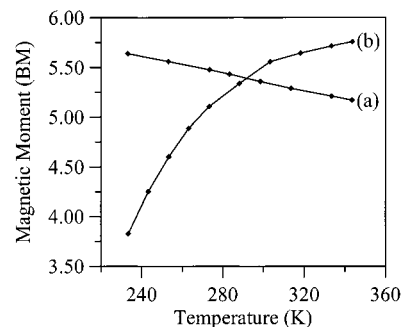


**Figure 12.** Variation of solution magnetic moment (from the modified Evans method[26]) with temperature for (a) $[FeL_2](ClO_4)_2 \cdot CH_3CN$ and (b) $[FeL'_2](ClO_4)_2$.

explain the behavior on temperature variation by the simultaneous presence of LS and HS states, the latter dominating at higher temperature. Also, it is surprising to note that the line width in this case also increases on decreasing temperature, but generally the line width is less than that for $[FeL_2]^{2+}$. So we surmise that the line width effect here in $[FeL'_2]^{2+}$ is essentially due to viscosity. The NMR properties of the complex ion in $[FeL_2](BPh_4)_2 \cdot 2CH_3CN$ with the larger counterion $BPh_4^-$ or in $[FeL_2](PF_6)_2$ are identical to those of $[FeL_2](ClO_4)_2 \cdot CH_3CN$ indicating that only the "fluxional" behavior of $[FeL_2]^{2+}$ cation is responsible for their spectral manifestations. So, the thermally driven interconversion of spin forms is very much of an attribute to the $FeL_2^{2+}$ ion in both solid and solution states.

**Evans Method.** Variable-temperature $^1H$ NMR studies of $[FeL_2]^{2+}$ independent of the anion support increased populations of low-spin isomers on increasing temperatures though in the solid states there are additional contributions and restrictions from lattice packing and spin state. To gain additional support for the thermally driven interconversions we have also carried out susceptibility studies for all three complexes and for the normal spin crossover complex $[FeL'_2](ClO_4)_2$ in acetonitrile solution using the modified Evans method.[26] The plot of the effective magnetic moment in solution (Figure 12a) for $[FeL_2]^{2+}$ compounds in the temperature regime 233−343 K reveals that $\Delta\nu$, the chemical shift differences between the reference and the one in the complex, vary from 1059.0 Hz at 233 K to 626.5 Hz at 343 K. This corresponds to the change of magnetic moment from 5.63 $\mu_B$ at 233 K to 5.17 $\mu_B$ at 343 K. The definite and substantial decrease in magnetic moment on increasing the temperature is a positive indication of increased contribution of the low-spin conformer. The contribution from this isomer is expected to increase from 2 to 25% in the temperature region of 4.2 to 300 K for compound **1** and up to 40% in compound **3** according to the Mössbauer data. Hence, the results of Evans method reveal similar trends with the Mössbauer and magnetic susceptibility data in the solid state.

On the contrary, the magnetic susceptibility measurement by Evans method done on the normal spin crossover iron complex, $[FeL'_2](ClO_4)_2$, reveals that the magnetic moment increases from 3.8 $\mu_B$ at 230 K to 5.57 $\mu_B$ at 330 K (Figure 12b), as expected, due to increased population of the HS state at higher temperatures.

**Nature of Conformers in 1−3.** The compounds $[FeL_2]-(ClO_4)_2 \cdot CH_3CN$ and $[FeL_2](PF_6)_2$ appear to undergo a thermally driven interconversion between two forms, possibly from a *mer* to *fac* isomer or a boat to chair conformation with temperature, and the compound $[FeL_2](BPh_4)_2 \cdot 2CH_3CN$ undergoes a first-order structural change at ∼200 K in solid state as supported by detailed temperature-dependent Mössbauer spectral analysis

and susceptibility studies. Solution NMR studies of all complexes reveal an increased population of low-spin component due to the $FeL_2^{2+}$ ion with increasing temperatures. The SQUID susceptibility study of solid **1** and the NMR of isolated $FeL_2^{2+}$ by Evans method clearly show a decrease in their magnetic moment from 230 to 300 K. This testifies to our two-conformer or -isomer model (vide supra).

The differential behavior of **1** and **3** from **2**, the former giving rise to two definite conformers and the latter a structural phase transition, draws its support from the volume space available for one $FeL_2^{2+}$ entity in the unit cells. After deduction of the spatial volumes of the counterions and the solvent molecules, it is calculated that the space available for each $FeL_2^{2+}$ ion for its occupation and motional dynamics is 1009.74, 1164.17, and 996.9 Å$^3$ respectively in the crystals of **1**−**3**. The crystals **1** and **3** having almost the similar volume space available for the cation in their lattices give very similar Mossbauer properties. However, the much greater space availability for the same cation in **2** gives it more freedom to go from one high-spin to another high-spin form through a series of intermediates (three identified at 200 K by Mössbauer). Any transformation from boat to chair or *mer*-to-*fac* is expected to be easier with the availability of a larger volume space within the unit cell. Whatever may be the nature of transition, in view of the several species present at 200 K in **2** one among which having lower isomer shift points a tendency to go toward a low-spin form. We infer that the real intermediate is a possible low-spin species, which does not get stabilized in **2** due to the formation of a much more stable high-spin species. It is interesting to note the presence of another species at 200 K with a very high $\Delta E_Q$ and the normal isomer shift value characteristic of a high-spin $Fe^{II}$. This again suggests a large structural change on its route. These transformations are possible in lattice **2** only due to the availability of a much larger volume space of 160 Å$^3$ more per cation in comparison to **1** and **3**. The similar Mössbauer properties of **1** and **3** make us conclude that such large scale structural changes are restricted by lower volume space available for the cation; hence, the temperature-dependent transformations gets stopped at an intermediate state level. The geometry restriction in molecules, if any in solution, is created by increased viscosity on lowering the temperature. Under such a suggested change, one particular ligand arrangement can provide for higher ligand field to create the low-spin state. This explains the temperature dependent population of both spin forms. This idea of molecular rearrangement of the ligand is supported by our dynamic NMR results on the diamagnetic $CuL^+$ species in solutions.[27,36] The unit cell of crystals **2** with tetraphenylborate anions with less closely packed $FeL_2^{2+}$ molecular species has more space to accommodate large-volume-requiring transformation as suggested above and hence could go through a full-scale *mer-to-fac* or chair to boat conformational change; in the process it could produce a few intermediates with changed molecular and hence electronic structures leading to differing isomer shift and quadrupole splitting values as observed by us. In this case while the room temperature form is of one type of high spin, the low-temperature (<200 K) form with slightly differing $\delta$ and $\Delta E_Q$ values should be another high-spin form.

One could question the coexistence of two forms in **1** and **3** since we observe only one kind of $FeL_2^{2+}$ structure in crystal structure. First it must be said that Mössbauer time scale is faster than that of X-ray and hence what we see as *mer* conformation in crystallography is essentially the time-averaged structure of the two conformers as we discussed under the Mössbauer

spectral section (vide supra). Such differences between Mössbauer (two $Fe^{II}$ states) and crystallography (single distinct $Fe^{II}$ site) do exist as has been well brought out in the case of Fe-[B(3-isopropylpyrazol-1-yl)$_4$]$_2$[38,39] and {Fe[HC(3,5-Me$_2$pz)$_3$]$_2$}-(BF$_4$)$_2$.[37] Apparently the high sensitivity of Mössbauer parameters to the local electronic environment of the $Fe^{II}$ ion is able to reveal subtle differences in the electronic and structural environment that are not apparent in the X-ray structural refinement.[41]

Yet another source to prove the presence of two forms is the very flexibility of the bis(pyrazolyl) ligand.[27,36,40] In an Fe(II) complex with a similar ligand, in which one of the two pyrazolyl groups contains only protons instead of methyl groups,[42] the ligands adopt a *mer* conformation about the metal atom so that the complex cation has no overall symmetry; this configuration leads to reduced interligand interaction. What is important to note is that the quality of the X-ray data was rather poor at 296 K and the structure had to be done[42] at 173 K. Furthermore in this compound at 173 K, the average iron−pyridine bond lengths are much longer than those in [FeL$_2$]$^{2+}$ lattice at RT reported here. Similarly, Fe−N(pyridine) − Fe−N(pyrazole) is 0.1 Å in this compound, while in ours the same is only 0.04 Å. Such disorders and differences in crystallography, observation of scattering of the susceptibility data for **1** in the temperature region of 120−200 K and the finding of a structural phase transition in **2** at 200 K are all due to the motional dynamics of the ligand. It must be said that the dynamic NMR of $Cu^I$ complexes of these ligands,[36] the presence of low-lying excited states in exchange coupled $Cu^{II}$ dimers containing these ligands,[40] and, of course, this report are all manifestations of the temperature-dependent molecular dynamics of the ligand L. Though the ligand dynamics is highly relevant here, the influence of the counterions in crystal lattice packing also plays a significant role in amplifying or modulating the ligand dynamics.

Finally yet another distant possibility−the presence of a low-lying excited state with a different low-spin multiplicity in these compounds which can only be proved by calculations−cannot be ruled out though the present explanation through the mode of differing configurations of the ligand within the same lattice is definitely more convincing.

## Conclusion

Three iron(II) complexes, [FeL$_2$](ClO$_4$)$_2$·CH$_3$CN, [FeL$_2$]-(BPh$_4$)$_2$·2CH$_3$CN, and [FeL$_2$](PF$_6$)$_2$, with a common chromophore FeN$_6$ made by using the same ligand L (2,6-bis (3,5-dimethylpyrazol-1-ylmethyl) pyridine) with differing counterions show lattice-packing-dependent Mossbauer and magnetic properties. All of them appear to undergo conformational change as a function of temperature though the first and the third have a properties different from the second one. Equally interesting is the fact that when they are all brought into solution, they retain their property of conformational change, indicating that the entire dynamics is controlled by the ligand movement. Theoretical models and additional crystallographic work underway are expected to prove not only the part played by the ligand but also the nature of lattice packing including the void space present in each one of them.

(41) Reiff, W. M.; Long, G. J. In *Mössbauer spectroscopy Applied to Inorganic Chemistry*; Long, G. J., Ed.; Plenum: New York, 1984; Vol. 1, p 245.
(42) Mahapatra, S.; Butcher, R. J.; Mukherjee, R. *J. Chem. Soc., Dalton Trans.* **1993**, 3723.

**Supporting Information Available:** Three X-ray crystallographic files, in CIF format, are available. This material is available free of charge via the Internet at http://pubs.acs.org.

IC010655G